

1 Fluctuation of the PV array maximum power point voltage during irradiance 2 transitions caused by clouds

3 4 **Authors:**

5 Kari Lappalainen*, kari.lappalainen@tuni.fi, phone: +358401981511

6 Seppo Valkealahti*, seppo.valkealahti@tuni.fi, phone: +358408490915

7 *Tampere University, Electrical Engineering, P.O. Box 692, FI-33101 Tampere, Finland

8 9 **Abstract**

10
11 Photovoltaic (PV) arrays are prone to climatic changes of which solar irradiance and PV cell
12 temperature are the most important on PV power production point of view. In well-designed PV power
13 plants, such as in typical utility scale PV plants, operational conditions are quite stable and homogeneous
14 apart from the fast irradiance transitions caused by cloud shading. These shading transitions cause fast
15 power fluctuations leading even to stability and quality problems in power networks. Fast non-
16 homogeneous irradiance transitions cause also mismatch losses in PV generators and the occurrence of
17 multiple maximum power points (MPP), which appear in a wide voltage range of the PV generator. In
18 consequence, the global MPP can fluctuate in a wide voltage region causing possible MPP tracking
19 problems and power losses. This article presents a study of the behaviour of the global MPP voltage of
20 various PV array configurations during irradiance transitions caused by clouds. The global MPP voltage,
21 its rate of change and the differences in voltage and available energy between the global MPP and the MPP
22 with the largest voltage of the PV generators have been analysed comprehensively, for the first time, by
23 using the characteristics of around 8000 measured irradiance transitions.

24
25 **Keywords:** Photovoltaic power generation; Maximum power point voltage; Irradiance transition; Partial
26 shading; Multiple maximum power points

27 28 **1. Introduction**

29
30 Partial shading of a photovoltaic (PV) system leads to conditions under which the PV cells of the
31 system receive non-homogeneous irradiance levels. Under homogeneous operating conditions, the non-
32 linear electrical characteristic of a PV array has only one maximum power point (MPP). However, under
33 non-homogeneous conditions, such as partial shading, the cells of a PV array have different electrical
34 characteristics leading to an aggregated electrical characteristic of the array. The shape of the current-
35 voltage ($I-U$) curve of the array varies rapidly and differs considerably from the shape of the traditional I -
36 U curve of a PV cell. Consequently, multiple MPPs can exist on the characteristic of the PV array and the
37 global MPP can vary over a wide voltage range. Therefore, partial shading affects largely on the operation
38 of PV systems causing, e.g., mismatch losses and failures in MPP tracking (MPPT). Mismatch losses mean
39 the difference between the combined maximum power of individual PV modules of a PV array, as if they
40 were operating independently, and the maximum aggregated power of the array. Mismatch losses exist in
41 every PV system whenever the modules have different electrical characteristics and there is nothing one

42 do, in practice, to reduce them in an existing PV system. On the other hand, multiple MPPs and large
43 variation of the global MPP voltage emerge primarily only during large variation of irradiance over the PV
44 plant. This kind of situation can take place only because of irradiance transitions caused by clouds in a
45 well-designed PV plant.

46 Under uniform operating conditions, successful MPPT is simple to implement. However, under
47 partial shading conditions typical MPPT algorithms based on the hill climbing method can be easily trapped
48 at a local MPP [1]. In order to harvest as large output power as possible under partial shading conditions,
49 various more complex MPPT algorithms have been presented such as particle swarm optimisation [2,3],
50 artificial bee colony optimisation [4,5] and Fibonacci search algorithm [6]. MPPT algorithms use a defined
51 operating voltage range to ensure that the global MPP is reached under varying operational conditions.
52 Some MPPT algorithms need to scan over 80% of the entire voltage range [7]. MPPT algorithms with
53 reduced voltage search ranges have been investigated e.g. in [8-10]. For most commercial inverters, the
54 manufacturers have specified an allowable voltage range of proper operation. It is essential to know the
55 operational MPP voltage range of the installed PV array in order to adjust the voltage range of the inverter
56 properly.

57 Partial shading of large PV power plants results mainly from overpassing cloud shadows. Several
58 research groups have studied cloud shadings previously. Irradiance transitions resulting from moving
59 clouds have been studied in [11,12] and also a mathematical model for transitions has been presented and
60 validated in [11]. Further, the apparent velocity of cloud shadow edges, i.e., the component of cloud shadow
61 velocity normal to the shadow edge, has been exhaustively studied in [13]. When a shadow of a moving
62 cloud covers a PV array, the apparent speed of the shadow edge defines how fast the PV array becomes
63 shaded. Moreover, mismatch losses and output power variation of PV arrays during measured irradiance
64 transitions caused by moving clouds have been studied in [14,15], respectively. It was found in [14] that
65 the overall effect of mismatch losses caused by cloud shadows is less than 1% on the energy production of
66 PV arrays, indicating that the mismatch losses resulting from cloud shadings are not a significant problem
67 for large PV power plants.

68 The range of global MPP voltage under partial shading has been studied earlier based on random
69 irradiance values in [8-10] and based on irradiance measurements in [16]. However, only single strings of
70 series-connected PV modules were studied with 24 PV modules at maximum. It was found in [8-10] that
71 the maximum possible global MPP voltage of a PV string is less than 90% of the nominal open-circuit
72 (OC) voltage of the string and the minimum global MPP voltages can be very low. Additionally, the MPP
73 voltages of individual partially shaded multi-crystalline silicon PV modules have been studied in [17].
74 However, all these studies considered only small basic PV generator configurations and were typically
75 based on hypothetical assumptions related to shading transitions. An exhaustive study on the MPP voltage
76 behaviour of PV arrays based on measured irradiance transition caused by clouds has not been presented
77 earlier.

78 For the first time, a study is presented in this paper on the behaviour of the global MPP voltage of
79 various PV array layouts and electrical configurations during measured irradiance transitions caused by
80 cloud shadows. The verified mathematical model of irradiance transitions caused by moving clouds [11]
81 was utilised to characterise around 8000 measured transitions. Then, the experimentally verified simulation
82 model of a PV module [18] was utilized to calculate the electrical properties of PV arrays composed of 10,
83 15 and 20 parallel strings of 25 series-connected PV modules and 25 parallel strings of 15 series-connected

84 PV modules during the characterised shading transitions. Moreover, a total-cross-tied (TCT) electrical
 85 configuration of 10×25 PV module array was studied for completeness. These PV arrays provide a
 86 realistic view on the behaviour of PV arrays used even in utility scale systems and have still reasonable
 87 computational times with the great amount of measured data used in analyses. The results are relevant
 88 especially from the points of view of PV array and system design and MPPT algorithm development, when
 89 striving for higher overall efficiencies of PV systems. The research methods and used data are presented
 90 in Section 2, the results are presented and discussed in Section 3, and the main conclusions are provided in
 91 Section 4.

92

93 **2. Methods and data**

94

95 **2.1. Simulation model**

96

97 Submodule of a PV module was used as a basic simulation unit in this study. A PV submodule is
 98 the group of series-connected PV cells protected by a bypass diode. The simulations were conducted using
 99 an experimentally verified MATLAB Simulink simulation model based on the well-known one-diode
 100 model of a PV cell [18]. The relationship between the current I and voltage U of a PV submodule is

$$101 \quad I = I_{\text{ph}} - I_0 \left(e^{\frac{U+R_s I}{AN_s kT/q}} - 1 \right) - \frac{U + R_s I}{R_{\text{sh}}}, \quad (1)$$

102 where I_{ph} is the light-generated current, I_0 the dark saturation current, A the ideality factor, R_s the series
 103 resistance, T the temperature and R_{sh} the shunt resistance of the submodule. N_s is the number of PV cells
 104 in the submodule, k the Boltzmann constant and q the elementary charge. Bypass diodes were modelled
 105 using Eq. (1) with the assumptions that I_{ph} is zero, R_{sh} is infinite and the bypass diode temperature equals
 106 to the temperature of the PV cells.

107 The simulation model was adjusted to represent the NAPS NP190GKg PV modules used in the PV
 108 research plant of Tampere University of Technology (TUT) [19]. The electrical characteristics of these PV
 109 modules consisting of three submodules of 18 polycrystalline silicon PV cells are shown in Table 1 under
 110 standard test conditions (STC). The used parameter values for the submodules and bypass diodes are
 111 compiled in Table 2.

112

113 Table 1

114 Electrical characteristics of the NAPS NP190GKg PV module under STC.

Parameter	Value
$P_{\text{MPP, STC}}$	190 W
$I_{\text{MPP, STC}}$	7.33 A
$U_{\text{MPP, STC}}$	25.9 V
$I_{\text{SC, STC}}$	8.02 A
$U_{\text{OC, STC}}$	33.1 V

115

116 Table 2

117 Parameter values of the simulation model for the submodules of the NAPS NP190GKg PV module and the bypass diodes.

Parameter	Value
A	1.30
R_s	0.329 Ω
R_{sh}	188 Ω
I_0, bypass	3.20 μA

A_{bypass}	1.50
$R_{\text{s, bypass}}$	20.0 m Ω

2.2. PV arrays

Various PV arrays were considered in this study consisting of 10, 15 and 20 parallel strings of 25 series-connected PV modules. This string length is typical in PV arrays of large-scale PV power plants. In addition, an array consisting of 25 parallel strings of 15 series-connected PV modules was included in the study in order to further study the effect of array shape on the behaviour of the global MPP voltage. Series-parallel (SP) electrical PV array configurations were selected for the study since SP is the most common configuration in PV array installations. For completeness, the total-cross-tied electrical array configuration of 10×25 modules was also considered. TCT configuration, where groups of parallel-connected modules are also connected in series, was selected since it is frequently proposed for improving PV system performance [20–22]. The PV modules were installed at a 45° tilt angle with respect to the horizon side by side in straight lines from east to west in the strings having a gap of 2.0 m between the strings. The dimensions of the studied PV arrays consisting of the NP190GKg PV modules are compiled in Table 3.

Table 3
Numbers of PV modules, dimensions, diagonals and areas of the studied PV arrays.

Number of modules (parallel \times series)	Dimensions (m)	Diagonal (m)	Area (m ²)
10×25	25.0×36.9	44.5	921
15×25	38.5×36.9	53.3	1418
20×25	51.9×36.9	63.7	1915
25×15	65.4×22.1	69.1	1448

2.3. Irradiance transitions and the shading of a PV array

Irradiance transitions of cloud shadow edges were modelled mathematically using the equation

$$G(t) = \frac{G_{\text{us}} - G_{\text{s}}}{1 + e^{(t-t_0)/b}} + G_{\text{s}}, \quad (2)$$

where G is the irradiance, t is the time and G_{us} and G_{s} are the irradiances of an unshaded and fully shaded situation, respectively [11]. Parameter b is related to the sharpness of the transition and its sign determines whether the transition is increasing (rise) or decreasing (fall). Parameter t_0 adjusts the transition time defining the midpoint of the transition. The shading strength (SS) of an irradiance transition, i.e., the magnitude of an irradiance change with respect to G_{us} , is defined as

$$\text{SS} = \frac{G_{\text{us}} - G_{\text{s}}}{G_{\text{us}}}. \quad (3)$$

By exploiting Eq. (2), irradiance transitions can be defined with four independent variables: b , SS and the apparent speed and direction of movement [13,23]. The duration of an irradiance transition was calculated as a product of b and the experimental regression coefficient of 7.67 [23]. Since a partial shading event of the studied PV arrays resulting from an overpassing irradiance rise is symmetrical to an event resulting from a similar irradiance fall, the absolute values of parameter b for the identified irradiance transitions were used in the simulations.

153 In total 7880 shadow edges, 4046 rises and 3834 falls, were identified in four months (May–August
154 2013) of irradiance data measured by three irradiance sensors applying the method offered in [11] and their
155 apparent velocities were determined utilising the method offered in [13]. The used sensors S2, S5 and S6
156 of TUT solar PV power station research plant [19] were oriented nearly due south with a tilt angle of 45°.
157 A 40% limit for minimum acknowledged SS was applied in the identification of the shadow edges since it
158 has been shown in [11] that shadows with lower SS have only minor effects on the operation of PV strings.
159 The average values of SS, the apparent speed and the absolute value of b of the identified shadow edges
160 were 59.2%, 8.66 m/s and 1.91 s, respectively. The average length of the irradiance transition area,
161 obtained as the product of the apparent speed and the duration of the transition, was 112 m. The identified
162 shadow edges moved dominantly towards eastern directions.

163 A cloud shadow edge was assumed to be linear across a PV array and the apparent velocity of the
164 shadow edge was assumed to stay constant during each simulation period, which are reasonable
165 approximations. A investigated simulation period lasted from the moment when a shadow edge moved
166 over the first PV submodule of the array until the shadow edge had moved across the array, i.e., when all
167 the submodules were again uniformly shaded. The used simulation time steps was 0.1 s and the irradiance
168 at the centre of each submodule was used for the whole submodule during a time step. To simplify and
169 speed up the computation, the PV array was selected to be under STC before each irradiance fall and the
170 temperature of the submodules was selected to stay constant. Only minor changes in PV module
171 temperatures, having negligible effects on the electrical operation of the modules, take place during fast
172 irradiance transitions.

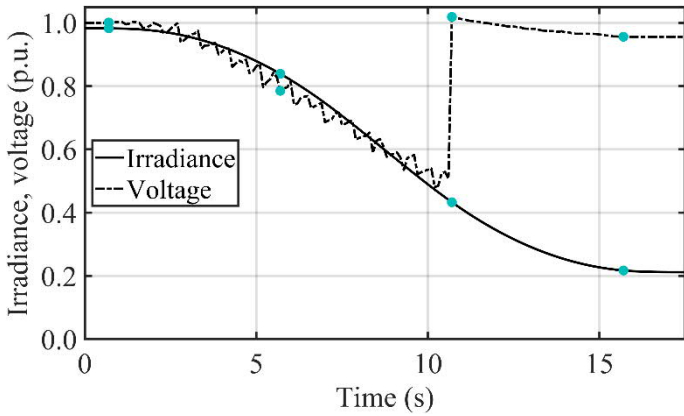
174 3. Results

176 For the first time, the MPP voltage behaviour during cloud shading of PV systems has been studied
177 comprehensively based on irradiance measurements. The global MPP voltage behaviour of the selected
178 PV arrays was studied during all the identified 7880 irradiance transitions. The results of the global MPP
179 voltage values are presented in Section 3.1 and their rate of change during the transitions in Section 3.2. It
180 was also calculated how much energy would be lost if the PV arrays would have operated at the largest
181 MPP voltage instead of the global MPP voltage. Moreover, the power and voltage differences between the
182 global MPP and the MPP with the largest voltage were calculated, as well as the range of the largest MPP
183 voltage. These results are presented in Section 3.3.

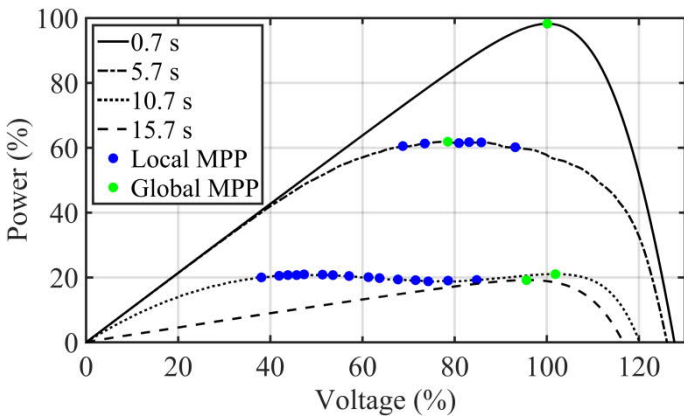
185 3.1. Global MPP voltage

187 The development of the $P-U$ curve of a PV array during irradiance transitions caused by a moving
188 cloud is illustrated in Figs. 1 and 2 by an example, where a sharp and dark shadow edge moves over the
189 10×25 SP array. It corresponds to the 95th percentile value of the SS (80.5%) and the 5th percentile values
190 of the apparent speed (2.97 m/s) and the absolute value of b (0.41 s) of all the identified shadow edges.
191 The apparent movement direction of the shadow edge was 45° with respect to the strings of the array. The
192 dots in Fig. 1 show four moments during the transition for which the $P-U$ curves are presented in Fig. 2.
193 The global MPP voltage is almost constant in the beginning of the transition and there is only one MPP
194 demonstrated by the first pair of dots in Fig. 1. When larger share of PV modules get partially shaded,

195 multiple MPPs exist in the $P-U$ curve of the array (the second pair of dots) over a wide voltage region and
 196 the global MPP voltage decreases down to 50% of the nominal MPP voltage of the array with increasing
 197 system shading until the MPP with the highest voltage becomes the global MPP (the third pair of dots).
 198 During this period, the global MPP voltage decreases almost in line with the decrease of the average
 199 irradiance. When the local MPP at highest voltage becomes the global MPP there is a leap in the global
 200 MPP voltage back to nominal MPP voltages of the array. The second lowest curve in Fig. 2 demonstrates
 201 this step. Thereafter, the global MPP voltage stays close to the nominal value of the PV array until the array
 202 is fully shaded. One should also note an interesting detail in Fig. 2 that the powers of the multiple MPPs
 203 are almost equal on the $P-U$ curves taken in the middle of the shading transition. This indicates that it might
 204 not be relevant, actually, to follow the global MPP during cloud shading transitions.
 205



206
 207 Fig. 1. Average irradiance and global MPP voltage of the 10×25 SP array during irradiance transition caused by a moving sharp shadow edge over the array.
 208 Irradiance is normalised to 1000 W/m^2 and voltage to the nominal MPP voltage of the array.
 209



210
 211 Fig. 2. $P-U$ curves of the 10×25 SP array at four moments (marked with green dots in Fig. 1) during irradiance transition caused by a moving sharp shadow
 212 edge over the array. Power is normalised to the nominal MPP power of the array.
 213

214 The ranges of the global MPP voltages for the studied PV arrays during the identified irradiance
 215 transitions are presented in Table 4. The maximum observed global MPP voltage for all the studied PV
 216 arrays was around 112% of the nominal MPP voltage (around 88% of the open circuit voltage) for the
 217 arrays. The result is in accord with Boztepe et al. [8], where the maximum global MPP voltage of a string
 218 of 20 PV modules was found to be 88.7% of the nominal open-circuit voltage. The smallest observed global
 219 MPP voltage was 28.0% of the nominal MPP voltage for the 10×25 SP array and around 30.5% for the
 220 15×25 and 20×25 SP arrays and the 10×25 TCT array. The range of the global MPP voltage was the

221 smallest with a lower limit of 39% for the 25×15 SP array, i.e., the array with the shorter string length. It
 222 is clearly smaller than for the 15×25 SP array of the same size, but having longer strings. The results mean
 223 that the number of parallel-connected strings and the electrical PV array configuration have only minor
 224 effects on the global MPP voltage range, only the string length has a visible effect to the smallest MPP
 225 voltages. These findings justify our reasoning that the results of this study are valid also for larger arrays
 226 of utility scale PV power plant having multitude of parallel connected strings.

227
 228
 229

Table 4
 Range of the global MPP voltage for the studied PV arrays during the identified irradiance transitions.

Array	Minimum voltage with respect to $U_{MPP,STC}$ (%)	Maximum voltage with respect to $U_{MPP,STC}$ (%)	Minimum voltage with respect to $U_{OC,STC}$ (%)	Maximum voltage with respect to $U_{OC,STC}$ (%)
SP, 10×25	28.0	112.0	21.9	87.6
SP, 15×25	30.5	111.9	23.9	87.5
SP, 20×25	30.4	111.9	23.8	87.5
SP, 25×15	39.4	111.6	30.8	87.3
TCT, 10×25	30.6	112.0	23.9	87.6

230

231 The relative cumulative frequencies of the global MPP voltage have been presented in Fig. 3 for
 232 the studied PV arrays during the identified shading transitions. It can be clearly seen that the global MPP
 233 voltage was most of the transition time near the nominal MPP voltage. The curve of the 25×15 SP array
 234 differs clearly from the others showing that the decrease of the PV string length decreases the overall
 235 deviation of the global MPP voltage from the nominal value. In particular, the proportion of time when the
 236 global MPP voltage was higher than the nominal voltage was smaller for the 25×15 SP array than for the
 237 others. This is in line that the range of global MPP voltage decreases with the decreasing length of PV
 238 strings (Table 4), which is plausible since short strings experience smaller irradiance difference than long
 239 strings during shading transitions caused by moving clouds. The curves of the other PV arrays
 240 configurations are close together showing that the global MPP voltage variation does not depend on the
 241 number of parallel connected strings or the electrical PV array configuration. The proportions of time when
 242 the global MPP voltages of the PV arrays were within 1%, 2% and 5% of the nominal MPP voltage during
 243 the identified irradiance transitions are presented in Table 5. The global MPP voltage was more than half
 244 of the time within 1% of the nominal value, over 70% of time within 2% and close to 90% of time within
 245 5%. These proportions of time were almost the same for the studied PV array configurations, except
 246 increased with decreasing string length. They demonstrate that the global MPP voltage is only small periods
 247 of time far from the nominal MPP voltage during the shading transitions. Actually, the global MPP voltages
 248 of the studied PV arrays were less than 95% of the nominal MPP voltage very rarely (Fig. 3). These findings
 249 have practical importance for the designing of PV systems and inverters used in them implying that a wide
 250 operational voltage range might not be needed because of the power losses caused by cloud shading.

251

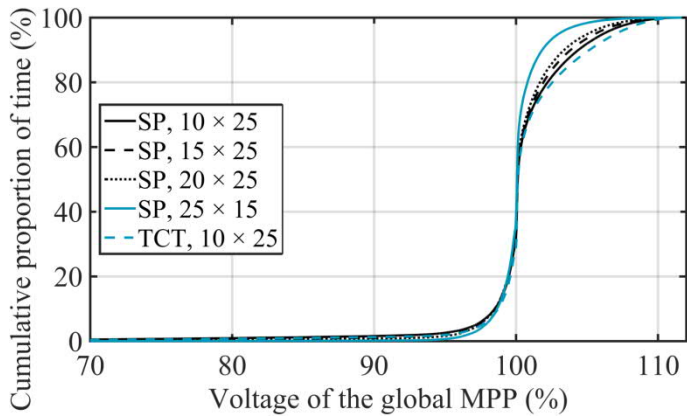


Fig. 3. Relative cumulative frequency of the global MPP voltage for the studied PV arrays during identified irradiance transitions.

Table 5

Share of time (%) when the global MPP voltages of the studied PV arrays was within selected limits from the nominal voltage during identified irradiance transitions.

Array	Within 1%	Within 2%	Within 5%
SP, 10 × 25	56.8	71.0	89.4
SP, 15 × 25	57.7	73.1	91.6
SP, 20 × 25	58.9	75.2	93.3
SP, 25 × 15	69.2	85.2	97.7
TCT, 10 × 25	57.1	70.6	87.6

3.2. Rate of change of the global MPP voltage

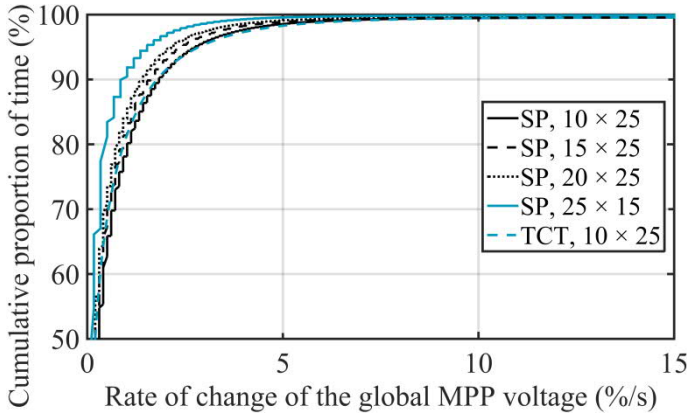
The average rates of change of the global MPP voltage during the identified irradiance transition due to clouds are presented in Table 6 for the studied PV arrays. The average rates of change were from 0.4 to 1.0 %/s being highest for the smallest 10 x 25 PV array configurations and smallest for the 25 x 15 configuration with shorter string length. It is noteworthy that the effect of the string length is much greater than that of the number of the strings. There was only minor difference in the average rate of change of the global MPP voltage between the TCT array and the corresponding SP array bringing forth that the TCT configuration does not provide extra value in response to added complexity of the array connections.

Table 6

Variation of the global MPP voltage for the studied PV arrays during the identified irradiance transitions with respect to the nominal MPP voltage.

Array	Average rate of change (%/s)	Maximum change during a time step (%)
SP, 10 × 25	0.99	75.6
SP, 15 × 25	0.82	71.1
SP, 20 × 25	0.70	71.4
SP, 25 × 15	0.40	67.1
TCT, 10 × 25	0.97	71.8

The cumulative frequencies for the rate of change of the global MPP voltage are shown in Fig. 4 for the studied PV arrays during the identified irradiance transitions. Most of the time the global MPP changed slowly and fast rates of change occur only seldom. For example, the rate of change of the global MPP voltage was half of the transition times smaller than 0.31 and 0.21 %/s for the 10 × 25 and 20 × 25 SP arrays, respectively, and over 5 %/s rates of change were very rare. The rate of change was almost equal for all the studied PV arrays, only somewhat smaller for the 25 × 15 SP array having shorter strings.



280
281 Fig. 4. Cumulative frequency of the rate of change of the global MPP voltage for the studied PV arrays during the identified irradiance transitions.
282

283 As presented in Fig. 1, an irradiance transition caused by a cloud may cause a large step on the
284 global MPP voltage when a local MPP near the nominal MPP voltage, caused by the fully shaded modules,
285 becomes the global one. In general, the largest changes (steps) occur when a local MPP at a different
286 voltage region than the global MPP becomes the global one. The largest changes of the global MPP voltage
287 during a simulation time step of 0.1 s are presented in Table 6. The largest observed change was over 75%
288 for the 10 × 25 SP array. The largest upward changes occur when a local MPP with a voltage near the
289 nominal MPP voltage becomes the global MPP as happened in the example of Figs. 1 and 2. For cases
290 where a shadow moves away from the array (irradiance rises), the situation is opposite. The largest
291 downward changes occur when a local MPP at low voltages becomes the global one when the global MPP
292 is near the nominal MPP voltage.

293 Large steps of the global MPP voltage may cause failures in MPPT and disturbances to the PV
294 inverter operation and to the output power of the PV plant. Therefore, a question arises on how often do
295 large voltage steps take place? During monotonic irradiance transitions, only one large step of the global
296 MPP voltage can exist as illustrated in Fig. 1. The proportions of the identified irradiance transitions, which
297 caused at least 5%, 20% and 40% global MPP voltage steps, are presented in Table 7. For the smallest
298 10 × 25 SP array, 10% of the irradiance transitions caused at least 5% steps on the global MPP voltage and
299 3% caused at least 40% voltage steps. The number of large steps decreased with the increasing number of
300 PV strings connected in parallel. For the 25 × 15 SP array, only negligible portion of the transitions caused
301 large voltage steps of practical importance. For the TCT array, the number of large voltage steps is actually
302 slightly higher than for the corresponding SP array. These results indicate that irradiance transitions caused
303 by moving clouds lead typically to quite small steps in the global MPP voltage on the point of view of
304 possible problems with MPPT and cause only minor losses for PV power plants equipped with proper
305 MPPT algorithms. However, voltage transition higher than 40% can take place few hundred times in four
306 months, i.e. few times in a day on the average. This might cause disturbances and quality problems for the
307 operation of the PV plant and to the output power.

308
309 Table 7

310 Proportions of the identified irradiance transitions (%), which caused larger steps of the global MPP voltage than the set limits. The voltage steps are with
311 respect to the nominal MPP voltage.

Array	At least 5%	At least 20%	At least 40%
SP, 10 × 25	9.89	6.65	3.15
SP, 15 × 25	8.22	5.37	2.44

SP, 20 × 25	7.01	4.35	2.06
SP, 25 × 15	1.59	0.55	0.22
TCT, 10 × 25	10.41	7.20	3.39

3.3. Operation at the largest MPP voltage instead of the global MPP voltage

The previously presented observations indicate that following the global MPP during irradiance transitions caused by clouds might not be very important on the point of view of energy harvesting. On the other hand, large variation of the inverter reference voltage caused by highly fluctuating global MPP voltage of the array during the transitions is a challenge for MPPT and can cause operational, power quality etc. problems. Therefore, it might be feasible to keep the inverter operational point at high voltages closer to the nominal MPP voltage all the time. This would make the PV system operation more straightforward and predictable. It might also decrease the need for a wide operational voltage range of PV inverters thereby increasing inverter efficiency. We have investigated the scenario of operating all the time at the largest MPP voltage close to the nominal MPP voltage in more details to get more insight to this issue.

The differences in the voltage, power and produced energy between the global and the largest MPP voltage for the studied PV arrays during all the irradiance transitions caused by clouds are shown in Table 8. The average and maximum differences in voltage are from 3.9% to 7.4% and from 68.5% to 75.7%, respectively, for the studied PV arrays in line with our earlier finding, naturally. However, the average differences in power are only between 0.7% and 1.4% although the maximum power differences during the transitions are even over 40%. Although the differences in voltage are distinct, the differences in power are quite small due to the flatness of the $P-U$ curves during the transitions as demonstrated already in Fig. 2. Only in some rare transition cases large differences can occur. The average differences in power decreased with the increasing number of the strings connected in parallel indicating that the increasing PV array size (area) smooths out irradiance fluctuations. Again, the decrease of the PV string length improved the PV system operation by decreasing the power differences and the TCT array configuration does not provide any actual benefit in terms of produced power or energy.

Table 8

Differences in the voltage, power and energy between the global and the largest MPP voltage for the studied PV arrays during the studied irradiance transitions. Differences in voltage and power are with respect to the nominal array values and difference in energy with respect to the energy produced at the global MPP.

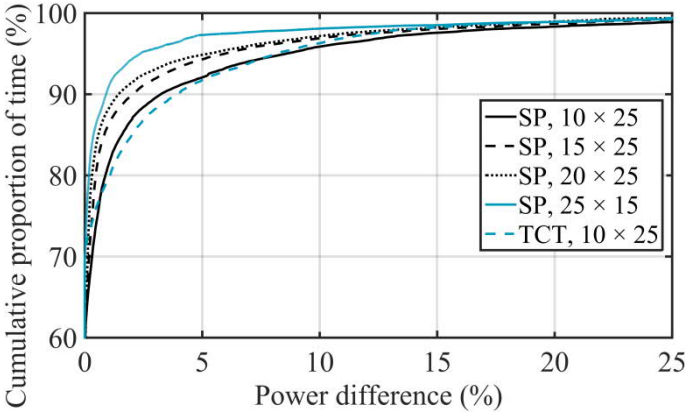
Array	Average difference in voltage (%)	Maximum difference in voltage (%)	Average difference in power (%)	Maximum difference in power (%)	Difference in produced energy (%)
SP, 10 × 25	7.44	75.7	1.41	42.9	0.14
SP, 15 × 25	6.32	73.3	1.08	43.2	0.09
SP, 20 × 25	5.80	73.4	0.95	42.5	0.07
SP, 25 × 15	3.87	68.5	0.69	35.6	0.02
TCT, 10 × 25	6.26	73.6	1.30	41.8	0.18

The difference in the produced energy between the global and the largest MPP voltage was only from 0.02% to 0.18% for the studied PV arrays. This means that only very small amount of energy is lost during the shading transitions if a PV generator is controlled to operate at the MPP with the largest voltage instead of the global one. It is noteworthy that the studied PV arrays had only one MPP over 90% of the time of the transitions and less than 10% of the time multiple MPPs. The difference in produced energy was the largest for the TCT array although the differences in voltage and power were smaller for the TCT array than for the corresponding SP array. The reason for this is that the proportion of time of having more

348 than one MPP was larger for the TCT array than for the others. For the SP arrays, the difference in produced
 349 energy decreased with increasing number strings connected in parallel and with decreasing length of the
 350 strings in line with earlier findings. It is also worth noting that only the time when the PV arrays were
 351 partially shaded due to clouds was studied. Therefore, the total difference in produced energy between the
 352 operation in the global MPP and in the MPP with the largest voltage is negligible.

353 In the example of Fig. 2, the MPP with the largest voltage is the global one in three cases out of
 354 four. In the case when the MPP with the largest voltage is not the global one (second highest curve in
 355 Fig. 2), the power difference between the global and the largest MPP voltage is 1.68% of the nominal
 356 power. Lost energy during the shading transition of the example would have been 2.38% if the PV
 357 generator had been operated at the MPP with the largest voltage instead of the global one. This kind of
 358 sharp irradiance transitions cause much higher irradiance differences for PV arrays than typical transitions
 359 and, thereby, bigger voltage and power difference between the global and the largest MPP voltages and
 360 larger energy losses. However, one must note that this kind of sharp irradiance transitions are quite rare
 361 and fast phenomena. They have negligible effect on the total energy production, but can cause momentary
 362 disturbances to the system.

363 For completeness, the cumulative frequencies of the power difference between the global MPP and
 364 the MPP with the largest voltage for the studied PV arrays during studied irradiance transitions are
 365 presented in Fig. 5. Most of the time, the power differences were very small being less than 5% more that
 366 90% of time for all arrays. No major differences of practical importance exist between the studied PV
 367 arrays.
 368



369 Fig. 5. Relative cumulative frequency for the power difference between the global MPP and the MPP with the largest voltage for the studied PV arrays during
 370 the irradiance transitions.
 371

372
 373 Based on the presented results, it is clear that the amount of energy lost when a PV array is operating
 374 at the MPP with the largest voltage instead of the global one is of no importance. Therefore, PV inverters
 375 could simply operate during the transitions at the largest MPP voltage, where inverter efficiency is also
 376 better. But does the voltage range of the largest MPP voltage differ much from that of the global MPP?
 377 The ranges of the largest MPP voltage of the studied PV arrays during the transitions are presented in
 378 Table 9. It is evident by comparing Tables 4 and 9 that the voltage range of the MPP with the largest voltage
 379 is clearly smaller than that of the global MPP. The minimum value of the largest MPP voltage was
 380 considerably larger and the maximum value slightly larger than the global MPP value for all the studied
 381 PV arrays. The voltage range also decreases with increasing number of the PV strings connected in parallel

and with decreasing length of the strings. All these findings justify the operation of PV generators at the MPP with the largest voltage, which has practical importance on the PV system control and design and on MPPT algorithm development.

Table 9
Range of the largest MPP voltage for the studied PV arrays during the irradiance transitions.

Array	Minimum voltage with respect to $U_{MPP,STC}$ (%)	Maximum voltage with respect to $U_{MPP,STC}$ (%)	Minimum voltage with respect to $U_{OC,STC}$ (%)	Maximum voltage with respect to $U_{OC,STC}$ (%)
SP, 10 × 25	49.8	116.7	39.0	91.3
SP, 15 × 25	55.5	116.6	43.4	91.2
SP, 20 × 25	58.4	116.1	45.7	90.8
SP, 25 × 15	74.5	115.4	58.2	90.3
TCT, 10 × 25	57.2	116.9	44.8	91.4

4. Conclusions

The behaviour of the global MPP voltage of various PV arrays has been studied in this article during irradiance transitions caused by moving clouds. SP and TCT arrays were studied having areas from 921 to 1915 m² containing from 250 to 500 PV modules. Both the number of series connected PV modules in the string and the number parallel connected PV strings were varied. The study was based on the characteristics of around 8000 measured irradiance transitions caused by moving clouds and was conducted using an experimentally verified one diode simulation model of a PV module and a mathematical model of irradiance transitions caused by moving clouds. The studied quantities were the values of the global MPP voltages and their rate of change during transitions. Also the power differences and lost energy were studied when the PV arrays were operated at the MPP with the largest voltage instead of the global one as well as the range of the largest MPP voltage. This is the first time when these quantities of PV arrays are studied comprehensively based on measured irradiance transition cause by clouds.

The global MPP voltage of the studied PV arrays varied between 28% and 112% of the nominal MPP voltage during the irradiance transitions. The number of parallel-connected strings and the electrical PV array configuration had only minor effects on the global MPP voltage range whereas the lower range values increased notably with decreasing string length. The average rates of change in the global MPP voltage during irradiance transitions were from 0.4 %/s to 1.0 %/s. The largest observed changes of the global MPP voltage during a simulation time step of 0.1 s were over 75%. They occurred when a local MPP at a different voltage region than the global MPP becomes the global one. However, only small portion of the irradiance transitions caused very large voltage steps so that these phenomena are not frequent.

The average differences in voltage and power between the global MPP and the MPP with the largest voltage were from 3.9% to 7.4% and from 0.7% to 1.4%, respectively. The differences decreased with the increasing number and decreasing length of the strings. The difference in available energy between the global MPP and the MPP with the largest voltage was negligible. The range of variation of the largest MPP voltage was clearly smaller than that of the global MPP voltage. These results justify the operation of PV arrays at the MPP with the largest voltage instead of the global one, which is valuable information for the design of PV inverters.

419 In overall, the behaviour of the PV array MPP voltage during irradiance transitions resulting from
420 cloud shadows causes only marginal problems to the operation and power production of the PV power
421 plants when proper MPPT algorithms are applied. The behaviour of MPP voltages of PV arrays during
422 irradiance transition caused by moving cloud shadows is now studied conclusively based on experiments.
423

424 **References**

- 425
- 426 [1] Esrām T, Chapman PL. Comparison of Photovoltaic Array Maximum Power Point Tracking
427 Techniques. *IEEE Trans. Energy Conversion* 2007;22:439–49.
 - 428 [2] Eberhart R, Kennedy J. A New Optimizer Using Particle Swarm Theory. In: *Proceedings of 6th Int.*
429 *Symp. On Micro Machine and Human Science*. p. 39–43.
 - 430 [3] Ishaque K, Salam Z. A Deterministic Particle Swarm Optimization Maximum Power Point Tracker
431 for Photovoltaic System Under Partial Shading Condition. *IEEE Trans. Industrial Electronics*
432 2013;60:3195–206.
 - 433 [4] Karaboga D, Ozturk C. A novel clustering approach: Artificial Bee Colony (ABC) algorithm.
434 *Applied Soft Computing* 2011;11:652–7.
 - 435 [5] Sundareswaran K, Sankar P, Nayak PSR, Simon SP, Palani S. Enhanced Energy Output From a PV
436 System Under Partial Shaded Conditions Through Artificial Bee Colony. *IEEE Trans. Sustainable*
437 *Energy* 2015;6:198–209.
 - 438 [6] Ahmed NA, Miyatake M. A novel maximum power point tracking for photovoltaic applications
439 under partially shaded insolation conditions. *Electric Power Systems Research* 2008;78:777–84.
 - 440 [7] Ishaque K, Salam Z. A review of maximum power point tracking techniques of PV system for
441 uniform insolation and partial shading condition. *Renewable and Sustainable Energy Reviews*
442 2013;19:475–88.
 - 443 [8] Boztepe M, Guinjoan F, Velasco-Quesada G, Silvestre S, Chouder A, Karatepe E. Global MPPT
444 Scheme for Photovoltaic String Inverters Based on Restricted Voltage Window Search Algorithm.
445 *IEEE Trans. Industrial Electronics* 2014;61:3302–12.
 - 446 [9] Furtado AMS, Bradaschia F, Cavalcanti ME, Limongi LR. A Reduced Voltage Range Global
447 Maximum Power Point Tracking Algorithm for Photovoltaic Systems Under Partial Shading
448 Conditions. *IEEE Trans. Industrial Electronics* 2018;65:3252–62.
 - 449 [10] Mäki A, Valkealahti S. Differentiation of Multiple Maximum Power Points of Partially Shaded
450 Photovoltaic Power Generators. *Renewable Energy* 2014;71:89–99.
 - 451 [11] Lappalainen K, Valkealahti S. Recognition and modelling of irradiance transitions caused by moving
452 clouds. *Sol. Energy* 2015;112:55–67.
 - 453 [12] Tomson T. Transient processes of solar radiation. *Theoret. Appl. Climatol.* 2013;112:403–8.
 - 454 [13] Lappalainen K, Valkealahti S. Apparent velocity of shadow edges caused by moving clouds. *Sol.*
455 *Energy* 2016;138:47–52.
 - 456 [14] Lappalainen K, Valkealahti S. Photovoltaic mismatch losses caused by moving clouds. *Sol. Energy*
457 2017;158:455–61.
 - 458 [15] Lappalainen K, Valkealahti S. Output power variation of different PV array configurations during
459 irradiance transitions caused by moving clouds. *Applied Energy* 2017;190:902–10.

- 460 [16] Mäki A, Valkealahti S. Effect of PV power generator layout on the global MPP voltage range during
461 cloud shading events. In: Proceedings of 28th European photovoltaic solar energy conference. p.
462 4063–70.
- 463 [17] Paraskevadaki EV, Papathanassiou SA. Evaluation of MPP Voltage and Power of mc-Si PV Modules
464 in Partial Shading Conditions. IEEE Trans. Energy Conversion 2011;26:923–32.
- 465 [18] Mäki A., Valkealahti S, Leppäaho J. Operation of series-connected silicon-based photovoltaic
466 modules under partial shading conditions. Progress in Photovoltaics: Research and Applications
467 2012;20:298–309.
- 468 [19] Torres Lobera D, Mäki A, Huusari J, Lappalainen K, Suntio T, Valkealahti S. Operation of TUT
469 solar PV power station research plant under partial shading caused by snow and buildings.
470 International Journal of Photoenergy 2013:837310.
- 471 [20] Belhachat F, Larbes C. Modeling, analysis and comparison of solar photovoltaic array configurations
472 under partial shading conditions. Sol. Energy 2015;120:399–418.
- 473 [21] Rakesh N, Madhavaram TV. Performance enhancement of partially shaded solar PV array using
474 novel shade dispersion technique. Frontiers in Energy 2016;10:227–39.
- 475 [22] Villa LFL, Picault D, Raison B, Bacha S, Labonne A. Maximizing the Power Output of Partially
476 Shaded Photovoltaic Plants Through Optimization of the Interconnections Among Its Modules. IEEE
477 Journal of Photovoltaics 2012;2:154–63.
- 478 [23] Lappalainen K, Valkealahti S. Mathematical parametrisation of irradiance transitions caused by
479 moving clouds for PV system analysis. In: Proceedings of 32nd European photovoltaic solar energy
480 conference. p. 1485–9.